Journal of Solid State Chemistry 208 (2013) 43–49

Contents lists available at ScienceDirect

Journal of Solid State Chemistry

journal homepage: www.elsevier.com/locate/jssc

Localization of vacancies and mobility of lithium ions in Li_2ZrO_3 as obtained by $^{6,7}Li$ NMR

Ya. V. Baklanova [a,*], I. Yu. Arapova [b], A.L. Buzlukov [b], A.P. Gerashenko [b], S.V. Verkhovskii [b], K.N. Mikhalev [b], T.A. Denisova [a], I.R. Shein [a], L.G. Maksimova [a]

[a] Institute of Solid State Chemistry, Ural Branch of the Russian Academy of Sciences, 91 Pervomaiskaya str., 620990 Ekaterinburg, Russian Federation
[b] Institute of Metal Physics, Ural Branch of the Russian Academy of Sciences, 18 Kovalevskaya str., 620990 Ekaterinburg, Russian Federation

ARTICLE INFO

Article history:
Received 5 March 2013
Received in revised form
11 June 2013
Accepted 20 September 2013
Available online 2 October 2013

Keywords:
Lithium zirconate
$^{6,7}Li$ NMR
Ab initio EFG calculations
Ion mobility

ABSTRACT

The $^{6,7}Li$ NMR spectra and the ^{7}Li spin–lattice relaxation rate were measured on polycrystalline samples of Li_2ZrO_3, synthesized at 1050 K and 1300 K. The ^{7}Li NMR lines were attributed to corresponding structural positions of lithium Li1 and Li2 by comparing the EFG components with those obtained in the first-principles calculations of the charge density in Li_2ZrO_3. For both samples the line width of the central ^{7}Li transition and the spin–lattice relaxation time decrease abruptly at the temperature increasing above ~500 K, whereas the EFG parameters are averaged ($\langle\nu_Q\rangle$=42 (5) kHz) owing to thermally activated diffusion of lithium ions.

1. Introduction

High thermal stability and chemical inertness against lithium of Li_2ZrO_3 put these ceramics to practical use as an effective reversible solid sorbent of CO_2 at 700–900 K [1–5], and as a promising candidate tritium breeding material for a D–T fusion power plant blanket [6–8]. Li_2ZrO_3 is also known as solid electrolyte (lithium-cation conductor) [9–11], which can be used for a protective coating of the silicon-based anode materials [12].

The crystalline Li_2ZrO_3 has two structural modifications [13–16]. The metastable tetragonal modification is formed at 750–1000 K and converts during annealing above 1070 K into a stable polymorph having the monoclinic structure up to the melting temperature ~1900 K. The most of studies deal with monoclinic lithium zirconate, which is synthesized in the high-temperature phase (HT) at $T_{syn} > 1300$ K. However, recently a substantial interest was focused on the low-temperature (LT) phases of the lithium metallates owing to their high reactivity [17,18]. In particular, only the lithium zirconate with T_{syn}=(1050–1300) K allows to obtain crystalline oxyhydroxides of the composition $ZrO(OH)_2$ by the lithium-hydrogen ion exchange in acetic [19] or nitric [20] acids. Unfortunately, an influence of T_{syn} on physical and chemical properties of the monoclinic lithium zirconate remains still very scanty [4,19,20].

An application in advanced technologies gives rise to key issues related to real local structure and microscopic mechanisms of cation transport in this material. The limited data on the structural imperfections in the lithium sublattice are of particular concern. In monoclinic Li_2ZrO_3 (space group $C2/c$) there are two structural lithium sites, Li1 and Li2, which six-fold octahedral oxygen coordinations are distinctly deformed. As shown in Fig. 1, the edge sharing along *b*-axis $(Li1)O_6$ octahedra forms in the *ac* plane the mixed metal $(Li–Zr)O_6$ bilayers, which are separated with layers of the $(Li2)O_6$ octahedra. According to X-ray and neutron diffraction study of the monoclinic lithium zirconate [16], with heating from room *T* up to ~800 K the LiO_6 octahedron is deforming substantially for the Li1-sites in the mixed (Li,Zr) layer while the six-fold oxygen coordination of Li2 remains almost without change. Such anisotropic change of the Li–O bond length leads to a redistribution of lithium among Li1 and Li2 sites with preferable localization of vacancies at Li1 sites inside the most distorted octahedrons. To explain an ionic conductivity jump above 700 K it was assumed [11,16] that a network of the distorted $(Li1)O_6$ octahedrons can stimulate diffusion of lithium in the $(Li–Zr)O_6$ layer by hopping from octahedral to octahedral site through intermediate tetrahedral sites [21–22]. On other hand, it was revealed in the recent 2D ^{6}Li NMR experiments [23] the diffusion of lithium ions is determined exclusively by two-site exchange Li1–Li2 with the extremely low atomic frequency hopping (about 60 jumps/h) near room temperature.

While a fast thermally activated Li mobility was directly evidenced by ^{7}Li NMR in the high temperature range [11], the pathway of Li-jumps remains in question. The main task of our research is to study the mechanisms of lithium diffusion at temperatures, as closer as possible to the operating range, (300–800) °C, of the suggested practical applications. ^{6}Li solid state

* Corresponding author. Tel.: +7 3433623529.
E-mail address: baklanovay@ihim.uran.ru (Ya.V. Baklanova).

0022-4596/$ - see front matter © 2013 Elsevier Inc. All rights reserved.
http://dx.doi.org/10.1016/j.jssc.2013.09.030

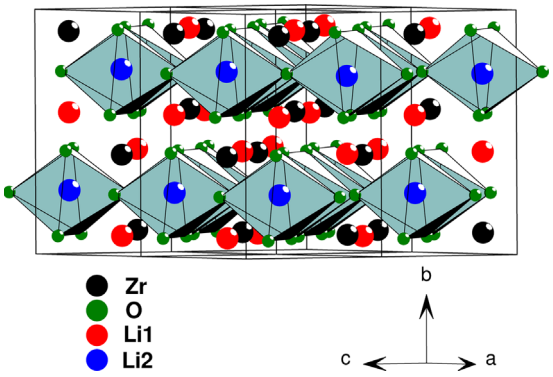

Fig. 1. Crystal structure of monoclinic Li_2ZrO_3.

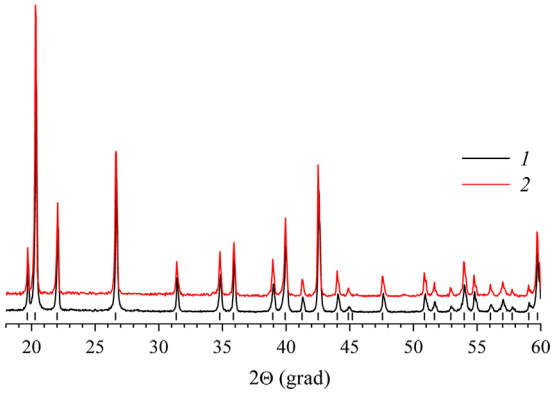

Fig. 2. X-ray powder diffraction pattern of LT-LiZr (1) and HT-LiZr (2) samples.

magic angle spinning (MAS) and ^{7}Li static NMR spectroscopy were used to investigate the localization of Li vacancies and their redistribution with temperature up to 900 K in the polycrystalline Li_2ZrO_3 samples, which monoclinic structure was stabilized by annealing at two distinct temperatures. One of the samples was synthesized near the low-*T* boundary of the monoclinic phase at $T_{ann}=1050$ K, and another sample was prepared under conventional conditions of the HT-synthesis, at $T_{ann}=1300$ K. The electric field gradient (EFG) was evaluated for both Li sites by analyzing the quadrupolar splitting of ^{7}Li NMR spectra. The ^{7}Li NMR lines were attributed to corresponding structural positions of lithium by comparing the EFG tensor components with those are estimated from an *ab initio* calculations of the charge density in monoclinic structure of Li_2ZrO_3. Moreover, an intrinsic correlation, existing between the ^{6}Li chemical shift and the lithium coordination [24], is suggested to provide unambiguous correspondence between structural sites of lithium and ^{6}Li NMR.

2. Experimental

Zirconium hydroxide carbonate $Zr(OH)_2CO_3{\cdot}5.5–6.0\cdot H_2O$ (99.9%) and lithium carbonate Li_2CO_3 (99.9%) were used as initial reagents to produce lithium zirconate Li_2ZrO_3. The compounds taken in stoichiometric amounts were dissolved in nitric acid HNO_3. Then the as-prepared solution was evaporated at 520 K to remove excessive nitric acid, and powder-like citric acid $C_6H_8O_7\cdot 2H_2O$ was added in the amount sufficient for the formation of the citrate complex of Zr(IV). The solution was evaporated until a dry residue was formed, which was then stepwise annealed at temperatures 600–1050 K (low-temperature phase Li_2ZrO_3—sample LT-LiZr) and 600–1300 K (high-temperature phase Li_2ZrO_3—sample HT-LiZr). Synthesis of lithium zirconate by the citrate method was described in detail elsewhere [25]. Before examination, LT-LiZr and HT-LiZr samples were annealed for 3 h at 1050 K and 1300 K, respectively.

The chemical composition of the samples was determined by emission spectrum analysis (Zr content) on an Optima 4300DV device with inductively coupled plasma and by atomic absorption method in acetylene-air flame on a Perkin-Elmer 503 device (Li content). The error of determination of each element did not exceed 5% relative to a composition of the cations in the chemical formula Li_2ZrO_3. The X-ray powder diffraction patterns were collected with a Shimadzu 7000S diffractometer (Cu$K\alpha_1$-radiation) at room temperature. The Rietveld refinement procedure (the FULLPROF package [26,27]) was used to obtain crystalline lattice parameters. The phase purity of the samples was confirmed by comparing their XRD patterns with those in the PDF2 database (powder diffraction file, ICDD, USA, release 2010). According to XRD data (Fig. 2), Li_2ZrO_3 samples were indexed in the monoclinic system (S.G. *C*2/*c*) with lattice parameters (see Table 1) which are close to the published results [13]. Based on rather narrow Bragg peaks we may estimate the average size of crystallites more than 100 nm. No additional broadening of the Bragg peaks was detected by varying the annealing temperature of samples from 1050 K to 1300 K. To determine the particle sizes, the micro-images of examined species (Fig. 3) have been obtained by scanning electron microscopy JSM-639OLA (JEOL). With increasing T_{ann} the SEM images show slight coarsening of the particles without any change of their morphology. The particles of both samples have platelet shape and form agglomerates with the average particle size 0.4–0.8 μm and 1–1.5 μm for the LT-LiZr and HT-LiZr samples, respectively.

^{7}Li NMR measurements were carried out over the temperature range (300–900) K on an AVANCE III 500WB BRUKER spectrometer in magnetic field $H_0=11.74$ T. The static broad spectra of ^{7}Li (the nuclear spin $^7I=3/2$; quadrupole moment $^7Q=-0.04$ b) were obtained by means of nonselective excitation either of the free induction decay (FID) signal or of the spin echo signal with subsequent Fourier transformation of the acquired signals. The $\pi/2$ pulse length was 3.2 μs. A single rf pulse of 1.6 μs was used to excite the FID signal. The 16-fold phase (*X*,*Y*) cycling was applied for the pulse sequence $(\pi/2)_X-t-(\pi/3)_Y$ to accumulate the Solomon-type spin echo which allows to get the correct intensity ratio, 3: 4: 3, of the central ($m_I=-1/2-+1/2$) and the satellite ($m_I=\pm 1/2\leftrightarrow\pm 3/2$) lines in the quadrupolar split ^{7}Li spectrum [28,29]. Two subsequent acquisitions of the echo-signal were repeated in a time $\sim$(3–4) $^7T_1$, the ^{7}Li nuclear spin–lattice relaxation time. The obtained powder spectrum was simulated to quantify the quadrupole frequency, $\nu_Q=(3eQ/2I(2I-1)h)V_{ZZ}$, and an asymmetry parameter, $\eta=|(V_{XX}-V_{YY})/V_{ZZ}|$, of the EFG tensor, $\{V_{ii}\}$ at the distinct Li sites. The calculations imply both the first ($\sim\nu_Q$) and the second ($\sim\nu_Q^2/\nu_0$) order quadrupolar coupling corrections of the Zeeman splitting with $\nu_0=^7\gamma H_0/2\pi$ [30]. The final spectrum represents an average over all possible orientations of the crystallites.

The magic angle spinning (MAS) spectra of ^{6}Li ($^6I=1$; $^6Q=-0.0006$ b) were acquired with an AGILENT 400WB spectrometer operating at 9.4 T. The MAS experiments were performed using a 4 mm rotor with a spinning speed of about 10 kHz. The ^{6}Li spectra were referenced to 1 M LiCl solution ($\delta=0$ ppm).

3. Results and discussion

3.1. ^{6,7}Li NMR spectra and vacant structural positions of lithium at room temperature

In the monoclinic structure of lithium zirconate, the charge environment of Li has symmetry which is lower than cubic for both the Li1 and Li2 sites. In such a case the interaction of electric